Wavelength-dependent backscattering measurements for quantitative monitoring of apoptosis, Part 2: early spectral changes during apoptosis are linked to apoptotic volume decrease

Christine S. Mulvey
Kexiong Zhang
Wei-Han Bobby Liu
David J. Waxman
Irving J. Bigio

Wavelength-dependent backscattering measurements for quantitative monitoring of apoptosis, Part 2: early spectral changes during apoptosis are linked to apoptotic volume decrease

Christine S. Mulvey,[a] Kexiong Zhang,[b] Wei-Han Bobby Liu,[a] David J. Waxman,[b] and Irving J. Bigio[a,c]
[a]Boston University, Department of Biomedical Engineering, 44 Cummington Street, Boston, Massachusetts 02215
[b]Boston University, Department of Biology, 5 Cummington Street, Boston, Massachusetts 02215
[c]Boston University, Department of Electrical & Computer Engineering, 44 Cummington Street, Boston, Massachusetts 02215

Abstract. Elastic scattering spectroscopy (ESS), in the form of wavelength-dependent backscattering measurements, can be used to monitor apoptosis in cell cultures. Early changes in backscattering upon apoptosis induction are characterized by an overall decrease in spectral slope and begin as early as 10 to 15 min post-treatment, progressing over the next 6 to 8 h. The timescale of early scattering changes is consistent with reports of the onset of apoptotic volume decrease (AVD). Modeling cellular scattering with a fixed distribution of sizes and a decreasing index ratio, as well as an increased contribution of the whole cell to cellular scattering, resulting from increased cytoplasmic density, is also consistent with observed spectral changes. Changes in ESS signal from cells undergoing osmotically-induced volume decrease in the absence of apoptosis were similar, but smaller in magnitude, to those of apoptotic cells. Further, blockage of Cl^- channels, which blocks AVD and delays apoptosis, blocked the early scattering changes, indicating that the early scattering changes during apoptosis result, at least partially, from AVD. Work continues to identify the additional sources of early spectral scattering changes that result from apoptosis induction. © *2011 Society of Photo-Optical Instrumentation Engineers (SPIE).* [DOI: 10.1117/1.3644911]

Keywords: backscattering; spectroscopy; fiber optic sensors.

Paper 11401R received Jul. 25, 2011; revised manuscript received Sep. 5, 2011; accepted for publication Sep. 8, 2011; published online Oct. 28, 2011.

1 Introduction

The term apoptosis was first used in a now-classic paper by Kerr et al. in 1972 to describe a morphologically distinct form of cell death.[1] The role of apoptosis in a number of disease states, particularly in the treatment of cancer, provides motivation for development of a method to noninvasively detect and monitor this form of cell death. Developing tumors down regulate apoptosis pathways via what is considered one of the fundamental hallmarks of cancer.[2] Apoptosis can be increased in tumors responding to well-established treatment modalities, including radiation and photodynamic therapy.[3,4] Further, many cytotoxic anticancer agents induce apoptosis.[5–7] Enhanced apoptosis may also contribute to some of the adverse effects of chemotherapy.[3] It is thus highly desirable to have a noninvasive method to detect and monitor apoptosis in patients undergoing conventional cancer treatments, as well as for the development and testing of new drugs.[8] Such method would complement *in vitro* apoptosis measurements widely used in early-stage testing of new anticancer drugs.

Apoptosis is characterized by a number of unique morphological and biochemical changes that are the basis for current methods of detecting apoptosis in cell cultures. In the earliest stage of apoptosis, cells undergo apoptotic cell shrinkage, known as apoptotic volume decrease (AVD), with little or no change in the structure of intracellular organelles.[9] AVD precedes most other morphological and biochemical alterations associated with apoptosis[10] including DNA laddering, caspase activation, cytochrome c release, and exposure of phosphatidylserine (PS) at the cell surface.[11] AVD is accomplished by release of intracellular ions, particularly K^+ and Cl^-, and the osmotically obliged water,[12] in both intrinsically- and extrinsically-induced apoptosis.[11] AVD is an active process requiring energy, and it plays an active and critical role during cell death. AVD affects apoptotic nucleases as well as the activation of caspases.[13]

Molecular changes in mitochondria leading to caspase activation also occur at an early point during apoptosis. These events include the release of mitochondrial proteins and changes in ion and electrochemical gradients.[14] Remodeling of mitochondrial christae precedes cytochrome c release.[15] Christae remodeling in the absence of mitochondrial swelling can occur quickly, within 2 to 5 min from the time of apoptosis induction.[16] Many of the later biochemical and morphological changes in apoptosis that are detected optically, including chromatin condensation, result from the caspase activation.[17] Those later changes are discussed in the companion publication to this paper.

Current methods of detecting apoptosis in cell cultures exploit the unique biochemical and morphological hallmarks of apoptosis. However, all well-established methods of *in*

Address all correspondence to: Christine Mulvey, Boston University, Department of Biomedical Engineering, 44 Cummington Street, Boston, Massachusetts 02215; Tel: 617 358 1519; E-mail: cmulvey@bu.edu.

vitro apoptosis detection require disruption of the culture's environment through either physical disruption or through the addition of an exogenous agent. The invasiveness of current detection methods render accurate time course measurements difficult, requiring a separate culture for each time point of interest. Recently, there has been interest in developing optical methods based on light scattering to study cells undergoing apoptosis.[18–23]

Elastic scattering spectroscopy (ESS) is an inherently non-invasive method for monitoring subcellular changes on an organelle level, and yields quantitative information when paired with an appropriate analysis algorithm.[24–26] Apoptosis is a good target for ESS measurements due to the significant morphology changes that characterize an apoptotic cell. Recently, our group showed that the morphology differences between apoptotic and normally propagating populations of cells produce differences in both angularly- and wavelength-resolved scattering.[21, 22] We measured the angular dependence (phase function) of scattering from suspensions of Chinese hamster ovary (CHO) cells using a polar nephelometer, which can measure the scattering phase function over a 60 deg range of angles in ∼1 s.[27, 28] Phase-function measurements revealed differences in scattering as early as 10 min after the cells had been treated with the apoptosis inducer staurosporine, although the required suspension of cells renders the measurement technique nonideal for normally-adherent cell lines.[21] Instrumentation to measure the wavelength-dependence of scattering was designed for use with either plated or suspension cultures. Wavelength-dependent measurements in the near backward direction were also capable of discriminating between apoptotic and normally-propagating CHO cultures as early as 10 min post-treatment. This early optical signature is characterized by an overall decrease in spectral slope. The early time at which scattering changes are detectable following induction of apoptosis was initially somewhat surprising. It was assumed, perhaps naively, that the changes in scattering that were observed were based on nuclear changes, such as chromatin condensation, since those morphology changes are considerable, and the nucleus can contribute significantly to cellular scattering. Such changes, however, start later.[29, 30]

Initial attempts at explaining the slope change were based on extracting size distributions from those early-time-point measurements by modeling cellular scatterers with Mie theory. That analysis was consistent with a decrease in Rayleigh scatterers (<50 nm) and 150-nm scatterers, relative to control samples, and a corresponding increase in 200-nm scatterers, as relative contributors to the backscattering signal.[22] Although consistent, the explanation was deemed to be insufficient; hence, the study reported here. (Backscattering spectra at later times revealed a different, late optical signature, characterized by a slope increase for times later than 6 to 8 h.)

This combination of evidence sets the stage for the studies reported here. The literature reveals that the most widely reported apoptotic change that best matches our early time points of 10 to 15 min after treatment, is AVD. In the earliest stage of apoptosis, cells undergo apoptotic cell shrinkage, with little or no change in the structure of intracellular organelles.[9] AVD precedes most other morphological alterations during the apoptotic process,[10] including DNA laddering, caspase activation, cytochrome c release, and exposure of PS at the cell surface.[12] In particular, AVD

is an early event (<1 h) following staurosporine treatment,[31] preceding cytochrome c release and DNA laddering in multiple cell lines.[10]

This paper's companion publication presents the correlation of both early and late optical signals to the apoptotic process and addresses the origins of the late signal. The studies reported here were designed to elucidate the source(s) of the early optical signal, and to assess the role of AVD. As described below, results of experiments, theory, and modeling are consistent with the specific correlation of the early decrease in the spectral slope with AVD.

2 Modeling Methods and Experiment Design

2.1 *Method for Modeling of Scattering with Water Loss and a Fixed Organelle Size Distribution*

AVD invokes the loss of water from the cytoplasm, not accompanied by commensurate loss of ions or other dissolved/suspended matter. One consequence of this is an expected increase in the cytoplasmic index of refraction. To test the hypothesis that changing only the index of refraction of the cytoplasm could result in a change in scattering consistent with our early optical signal, a size distribution of scattering centers was extracted (using an inverse Mie theory formalism) from scattering measurements taken from a culture treated with staurosporine for 30 min and 4 h. As described in a previous publication, cells contain scatterers in a range of sizes that are distributed in a punctate manner, with large gaps between sizes.[22] To represent this distribution, fitting was performed with a small number of sizes, each representing a specific class of organelle: Rayleigh scatterers (10 nm), lysosomes and peroxisomes (150, 200, and 300 nm), mitochondrial widths (600 nm), mitochondrial lengths (1.4 μm), and nuclei (8 μm). Due to the high frequency oscillations present in the scattered spectrum of large particles, any variation in size would have a marked effect on the spectrum included for fitting. To represent the biological variability in the size of cell nuclei, a Gaussian size distribution with a 20% C.V. was included in the Mie theory prediction of 8 μm particles. Distribution effects are not as pronounced for smaller sizes and were therefore not included in this simulation. An index of refraction of 1.41 was used for the organelles, while 1.39 was used for the refractive index of the cytoplasm after water loss, resulting in an index ratio of 1.01.

Further, while under normal conditions, the contribution of whole cell scattering is small due to the small index mismatch between intracellular and extracellular fluids, as water is lost from the cell, the index mismatch across the cell membrane increases. This increase in index ratio should result in an increased contribution of the whole cell to cellular scattering. Moreover, during apoptosis, adherent cells also partially detach from the substrate, causing them to "round up." This effect is illustrated in Fig. 1. We postulate that these rounded-up cells may act more like scattering centers than those that remain attached to the plate, as relatively flat structures.[14, 32]

To simulate the effect of whole-cell scattering consequent to the increased refractive index of the cytoplasm, Mie theory was used to predict the scattering from a Gaussian distribution of cell-sized spheres (11.5 μm mean diameter, 20% C.V.) after cytoplasm condensation, with $n_{extracellular} = 1.35$ and $n_{intracellular} = 1.39$, corresponding to an index ratio of 1.03. The resulting
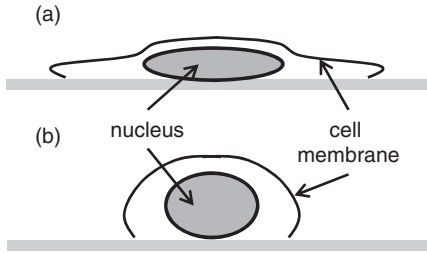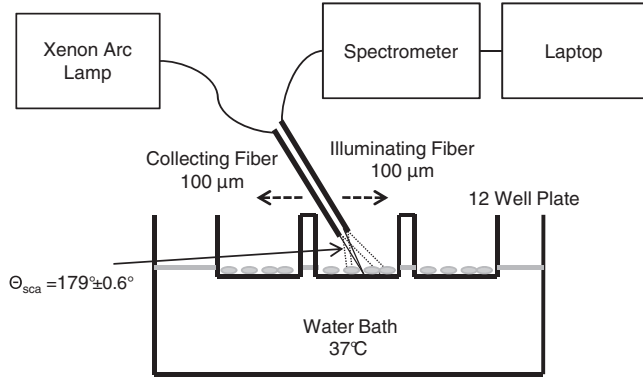
Fig. 1 (a) Adherent cells normally have a relatively flat structure, though (b) shows a loss of adherence during apoptosis results in a more round shape.

Fig. 3 A schematic of the system used to measure wavelength-dependent backscattering. A fiber probe, containing 100 μm fibers in a standard six-around-one geometry (for clarity, only one pair is illustrated), collects light scattered at approximately 179 deg from plated cell cultures. The cultures are grown in glass-bottomed 12-well plates and are positioned at the surface of a temperature-controlled water bath. The probe translates to access all 12 wells on the plate.

spectrum was included in the fitting matrix with the organelle spectra, for a total of eight possible sizes. For reference, the eight spectra used for fitting are presented in Fig. 2.

2.2 ESS Measurements

Wavelength-dependent measurements of scattering were made on cell cultures using instrumentation previously described elsewhere[22] and depicted in Fig. 3. In brief, broadband white light from a 150 W xenon short-arc lamp was delivered to and collected from a plated cell sample using a fiber optic probe consisting of seven 100 μm fibers — six illumination fibers surrounding a single collection fiber. For clarity of the figure, only one pair of illumination and detection fibers are shown. The cells were grown in glass-bottomed 12 well plates (Mat-Tek Corporation, P12G-1.5-14-F), which were placed on the surface of a temperature-controlled water bath. The tip of the fiber probe was positioned above the plate, at a distance of ~7 mm from the cell layer, such that the mean angle for collected light was 179.2 deg $\pm$ 0.6 deg. The unpolarized scattered light collected by the center fiber was transmitted to a spectrometer (Ocean Optics, USB4000) and analyzed. The probe's kinematic mounting system allows access to all 12 wells with precise repositioning.

Three separate spectral measurements, $I(\lambda)$, are required for each collected spectrum: the raw spectrum from the sample (I_{sample}), a background measurement ($I_{\text{background}}$) to account for any scattering from components other than cells, and a spectral response ($I_{\text{spec·resp.}}$), acquired with a spectrally-flat diffuse reflector (Spectralon, Labsphere, Inc.), to account for spectral characteristics of the system response.[22] The integration time for all sample and background measurements was 2 s, and the integration time for the spectral response was 10 ms, requiring each sample plate to be exposed to room air for no more than 3 min during measurements, with most of the time being used to maneuver the probe from well to well on the 12-well plate. Sample plates were returned to the incubator between measurements. The detector element of the spectrometer contains 2048 pixels, but to reduce pixilation noise, each measurement was smoothed with a eight-pixel boxcar corresponding to the
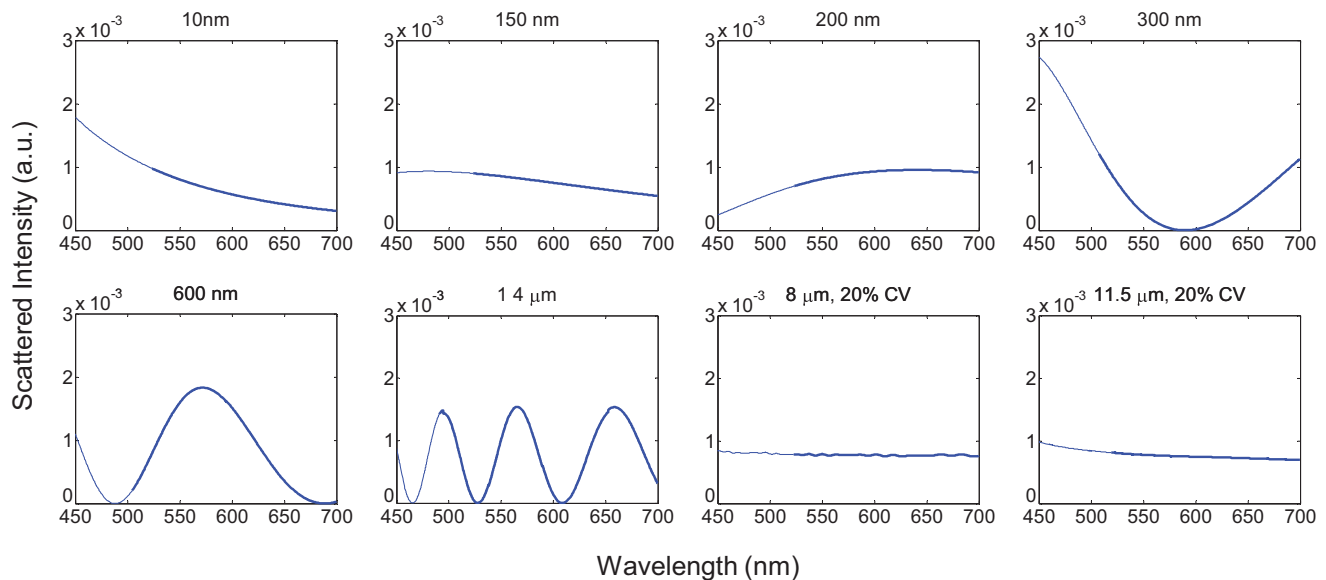
Fig. 2 Mie theory-predicted spectra present in the fitting matrix. The eight spectra correspond to single sizes of 10, 150, 200, 300, 600 nm, and 1.4 μm and two distributions of sizes of 8 and 11.5 μm mean diameter, both with 20% C.V.

resolution of the spectrometer (~1.5 nm). The scattered light spectrum from each sample was calculated with the following expression: $I_{\text{spectrum}} = (I_{\text{sample}} - I_{\text{background}})/I_{\text{spec.resp.}}$, and then normalized to the area under the curve. Measurements were made for the spectral range 450 to 700 nm.

2.3 *Volume Decrease in the Absence of Apoptosis*

To investigate cell volume decrease as the source of our early signal, cells were treated with differing concentrations of mannitol, a membrane-impermeable sugar alcohol, to increase the osmolarity of the medium and induce osmotic water loss. Three approaches were used to determine if the observed scattering spectral changes in apoptotic cells were consistent with the effects of volume decrease induced in a manner independent of apoptosis: caspase activity assay for apoptotic activity in cells treated with mannitol, quantification of the magnitude of volume loss by flow cytometry, and finally, scattering measurements made on the mannitol-treated cell cultures.

Osmotic volume loss was produced in CHO cultures by replacing the growth medium with fresh medium supplemented with one of the following: 50, 100, 200, 400, and 800 mm mannitol. The addition of these amounts of mannitol to isotonic growth medium (~295 mOsm/L) resulted in solutions with the following hypertonic osmolarities: 345, 395, 495, 695, and 1095 mOsm/L, respectively. The effects of mannitol on apoptosis were determined using a luminescent assay for effector caspase activity (Caspase-Glo 3/7 Assay, Promega, Inc.). Full details of this procedure are presented in this work's companion paper. Two treatment times were assessed: 4 and 24 h.

To assess the degree of volume loss that resulted from each concentration of mannitol, the forward scattering from each population was assessed in a flow cytometer. To prepare samples for flow cytometry, cells were plated in individual 35-mm polystyrene dishes and grown to confluence. At 30 min and 4 h, the growth medium was replaced by medium alone or medium supplemented with mannitol at the following concentrations: 50, 100, 200, 400, and 800 mm. Cells were washed twice with phosphate buffered saline (PBS) supplemented with the same concentration of mannitol as the treatment, the washes were collected for analysis, and the cells were incubated with Accumax (Innovative Cell Technologies) for 20 min to obtain single cell suspensions for flow cytometry. Following incubation, a small volume of the collected washes was added back to the plates and cell aggregates were disrupted by agitation. One percent formaldehyde fixation was used to prevent volume changes after the end of the treatment period due to resuspension in the isotonic buffer required for flow cytometry. The samples were kept on ice until flow cytometry was performed.

Backscattering measurements were made with the system described in Sec. 2.2, on confluent samples of CHO cells grown under standard conditions. At the beginning of the experiment, the growth medium was aspirated and replaced with clear Dulbecco's Modified Eagle's Medium (DMEM) supplemented with one of five different concentrations of mannitol: 50, 100, 200, 400, and 800 mm or with fresh DMEM. The three scattering measurements described in Sec. 2.2 were made before treatment, then at 15 min post-treatment, 30 min, 1, 2, 4, and 6 h to capture the onset and progression of changes in the optical signal during early apoptosis.

2.4 *Inhibiting Early Features of Apoptosis*

To determine whether the early optical signal is, at least partially, due to AVD, we investigated whether the signal is blocked when AVD induced by staurosporine is inhibited using the Cl$^-$ channel blocker 4,4′-diisothiocyanostilbene-2,2′-disulfonic acid (DIDS), which inhibits early manifestations of staurosporine-induced apoptosis.[42] Confluent cultures of CHO cells were treated with complete DMEM supplemented with one of the following: a control volume of 0.2% dimethyl sulfoxide (DMSO), 2 μm staurosporine in DMSO, 2 μm staurosporine in DMSO plus 200 μm DIDS, or 200 μm DIDS alone. The presence or absence of apoptosis in cultures treated with staurosporine or staurosporine plus DIDS was determined using the Caspase–Glo assay described in Sec. 2.3. At the beginning of the treatment period, the growth medium was replaced by growth medium supplemented with one of the following: 0.2% DMSO, 200 μm DIDS, 2 μm staurosporine, or 2 μm staurosporine plus 200 μm DIDS. Caspase activity was measured at 4 and 24 h following treatment.

To assess relative cell volume, cells were prepared for flow cytometry according to the protocol in Sec. 2.3. Each sample was treated with one of the following: 0.2% DMSO, 2 μm staurosporine in DMSO, or 2 μm staurosporine in DMSO plus 200 μm DIDS. Each sample was then washed and resuspended in isotonic PBS. Cell volumes were measured at 30 min and 4 h following treatment.

The three scattering measurements described in Sec. 2.2 were performed before treatment, then at 15 min post-treatment, 30 min, 1, 2, 4, and 6 h.

3 Results and Discussion

As a general reference, as reported in the companion paper, Fig. 4 shows a representative spectrum from an untreated culture (thin solid) along with spectra from apoptotic cultures exhibiting early-signal scattering changes at 4 h (thick solid) and late scattering changes at 24 h (thin dotted) after treatment with
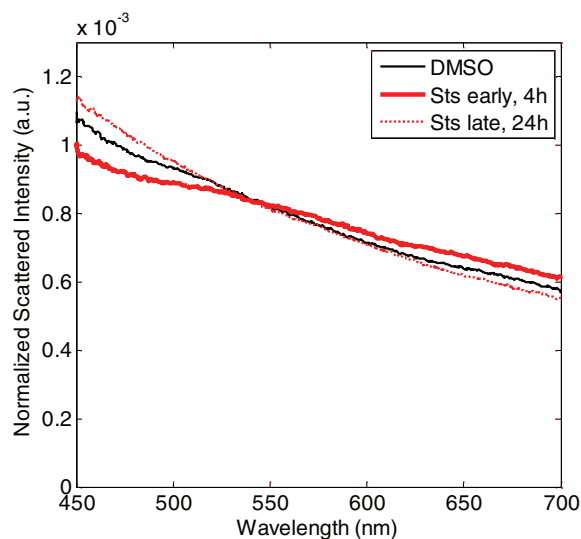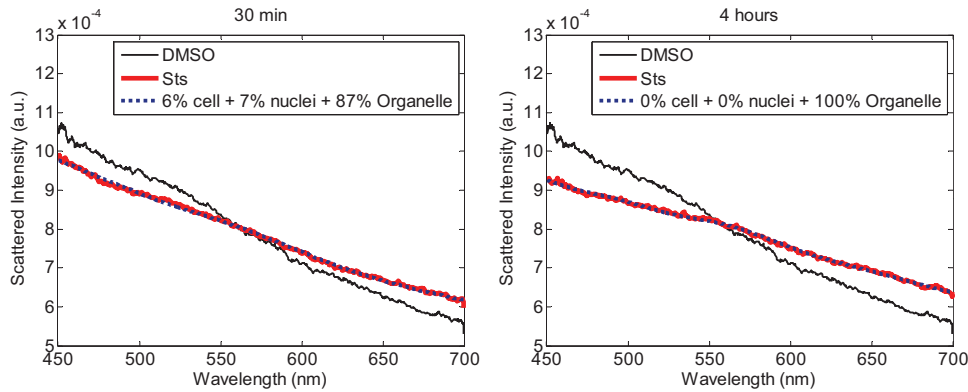
Fig. 4 Representative backscattered spectra from an untreated culture (thin solid) and a treated culture 4 h (thick solid) and 24 h (thin dotted) following apoptosis induction.

Fig. 5 The best-fit spectra (thick dotted) to ESS measurements of cultures treated with staurosporine (thick solid) for 30 m (left) and 4 h (right) using the Mie predictions shown in Fig. 2.

staurosporine. Time points as early as 30 min are similar to the 4-h time point shown here.

3.1 Modeling Water Loss with Mie Theory

To help quantify the effects of water loss on cellular scattering, a size distribution of scattering centers was extracted from ESS measurements taken on cell cultures treated with staurosporine. Size extraction was performed through least-squares fitting of the experimentally measured ESS spectrum to the wavelength-dependent Mie theory predictions for single particle sizes and the distributions of sizes described in Sec. 2.1 (see Fig. 2). Thirty minutes following apoptosis induction, when organelle-based morphology changes are expected to be minimal, the best fit spectrum to scattering from apoptotic cells (Fig. 5, left) is comprised of 6% contribution from the whole cell, 7% contribution from cell nuclei, and the remaining 87% results from other organelles. Each of the resulting contributions are reasonable and consistent with those in a cell before treatment occurs (data not shown), with most of the scattering due to the smaller subcellular structures, and modest scattering from the nuclei and the whole cell which are expected to scatter predominantly in the forward direction. This model fit suggests that backscattering measurements are sensitive to AVD at early times, with the increased contribution of the whole cell accounting for much of the scattering difference. Interestingly, at 4 h post-treatment (Fig. 5, right), while the cell has not regained any volume, the spectrum is comprised entirely of scattering from the smaller organelles. Currently, the reason for this is unknown, but may be a result of organelle-based apoptotic changes, including the loss of Rayleigh scatterers due to cytoskeletal breakdown, the remodeling of individual mitochondria as well as fragmentation of the mitochondrial network, or subtle changes in nuclear micromorphology due to chromatin condensation.

### 3.2 Inducing Volume Loss in the Absence of Apoptosis

To separate the effects of volume decrease itself from any associated apoptotic events, the level of apoptosis (caspase activity) was assayed at 4 and 24 h post-treatment for cells treated with each concentration of mannitol, used to induce apoptosis with minimal apoptosis. The average and range of values of three measurements are presented in Fig. 6.

The two lowest concentrations of mannitol produce caspase activity that is similar to the low level in the untreated control, and is significantly less than the level produced by staurosporine. From this we conclude that concentrations of 50 mm mannitol and 100 mm mannitol induce minimal apoptosis in CHO cells, and can be used to separate the optical effects of volume decrease from those of apoptosis.

To determine whether the strength of the early optical response correlates with the amount of volume decrease produced by treatment with hypertonic solutions of mannitol, the volumes
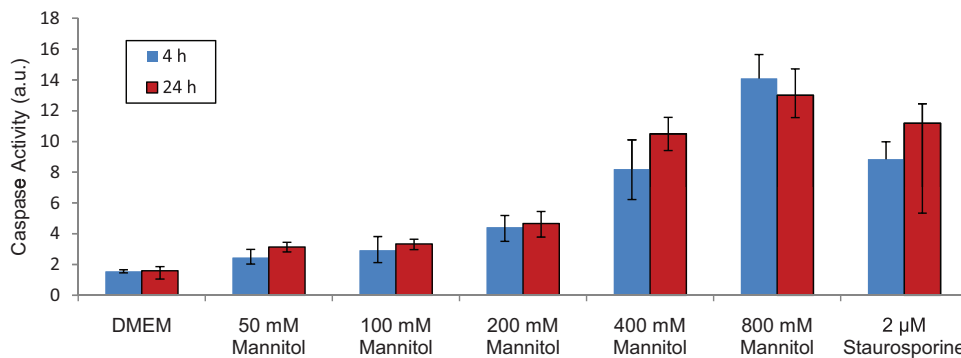
Fig. 6 Caspase-3 and caspase-7 activity in CHO cells treated with increasing concentrations of mannitol. The height of each bar is the average of the three measurements while the error bars span the range of measurements. The caspase activity of CHO cells treated with staurosporine is included for comparison.
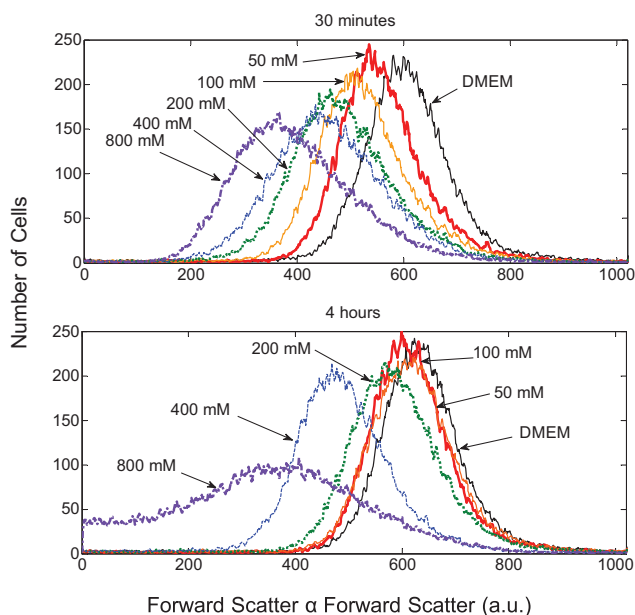
Fig. 7 Histograms of cell volume for CHO cells treated with increasing concentrations of mannitol as measured by flow cytometry.

Fig. 8 ESS data obtained from CHO cells treated with 50 mm (dashed line) and 100 mm (dotted line) mannitol for 1 h.

of these cell populations were measured with flow cytometry. The intensity of forward scattering was measured for 40,000 cells in each sample, and a histogram was generated. Histograms for cultures treated with five concentrations of mannitol and an untreated culture at each time point are overlaid in Fig. 7.

At 30 min of treatment, each of the cell populations treated with mannitol exhibited a shift to the left, indicating a decrease in mean cell volume. This decrease in volume is progressive with increasing concentration of mannitol. At 4 h post-treatment, the cells treated with 50 and 100 mm mannitol recovered much, but not all, of their volume, whereas the cells treated with 200 mm mannitol, have recovered only some of their volume by 4 h. In contrast, cultures treated with 400 and 800 mm mannitol did not exhibit any volume recovery, consistent with the high degree of apoptosis measured by caspase activity.

Scattering measurements were made on four sets of samples treated with varying concentrations of mannitol. The average spectra of the four trials from cultures treated with 50 mm (dashed) and 100 mm mannitol (dotted) for 1 h are plotted with the average spectrum of the untreated control (solid), in Fig. 8.

Before the samples were treated, they all produced nearly identical scattered spectra. Within 30 min of the addition of hyperosmotic medium, each sample showed changes in scattering consistent with the early optical signal produced by staurosporine treatment (similar to that shown in Fig. 4). As the concentration of mannitol increased, both the magnitude and the kinetics of the observed optical signal increased (not all data shown).

3.2.1 Discussion: mannitol produces similar early effects as staurosporine

Given that caspase activity is minimal in cultures treated with 50 and 100 mm mannitol (Fig. 6), it is possible to separate the optical effects of apoptosis from the effects of volume decrease in these populations. At early times, cells treated with higher concentrations of mannitol produce larger changes in scattering,
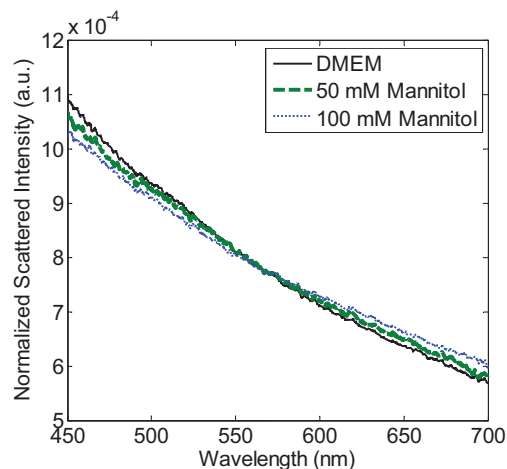
and this is consistent with a measured greater degree of volume loss.

After the initial shrinkage due to osmotic perturbation, viable cells can regulate their volume, to initial levels through regulatory volume increase (RVI). RVI is associated with NaCl influx with flow of osmotically obliged water.[10,33] Our volume measurements show that cells with small volume perturbations recover their initial volume after a transient period of shrinkage. A recovery to the untreated state is also evident in the scattering spectra. In the case of cells treated with 50 or 100 mm mannitol, the transient spectral change is reversed by 2 h and at some time between 4 and 6 h, respectively (data not shown). These timescales are consistent with volume recovery measured by flow cytometry. This suggests that the optical recovery seen in the cells not undergoing apoptosis is due to a recovery of volume, and that the early signal was due to volume loss.

Prolonged cell shrinkage by hypertonic stress that cannot be compensated for with RVI leads to apoptosis in many cell types.[12] One study found that experimental manipulations that reduce the cell volume to 70% of the original volume for periods of at least 3 h are sufficient to induce apoptosis.[34] In the case of CHO cells, cultures treated with both 400 and 800 mm mannitol exhibit significant volume loss without volume recovery (Fig. 6). The lack of volume recovery correlates with the persistence of the scattering changes as well as the presence of apoptosis in cells treated with mannitol at these concentrations.

Given that volume decrease in the absence of apoptosis produces scattering changes qualitatively similar to the early apoptotic signal, it is likely that the early optical signal observed upon apoptosis induction is due, in part, to volume loss.

We do note, however, that the magnitude of the optical response seen in the case of osmotically-induced water loss is not as large as that of the response produced by induction of apoptosis. Figure 9(a) compares the volume measurements of cells treated with 2 μm staurosporine and cells treated with 50, 100, and 800 mm mannitol. The ESS spectra from cultures incubated with mannitol are shown in Fig. 9(b), along with a spectrum from a culture treated to undergo apoptosis with staurosporine. While the addition of 50 mm mannitol produces a volume loss similar to that of the 2 μm staurosporine, the optical response
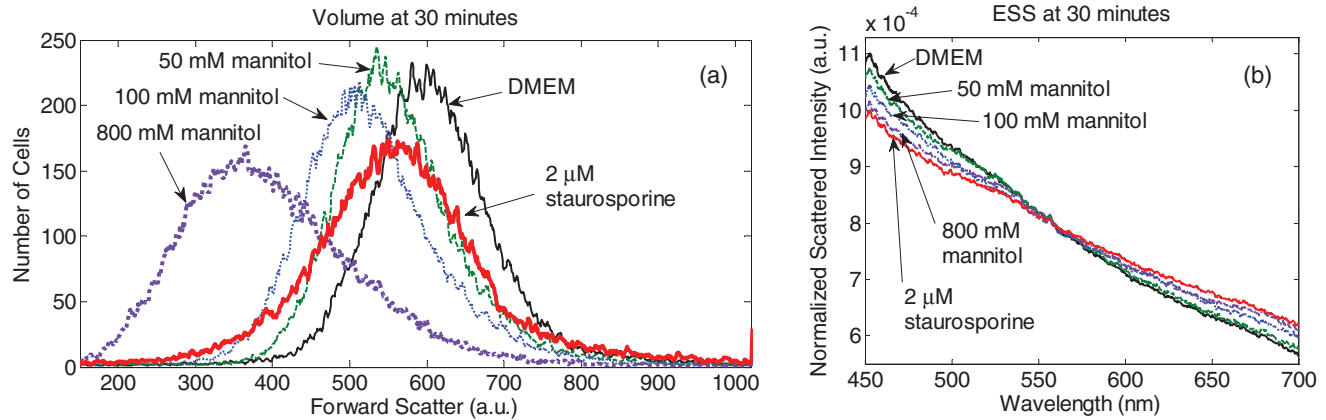
Fig. 9 (a) A comparison of volume lost upon apoptosis induction due to 2 μm staurosporine and osmotic stress produced by the addition of 50, 100, and 800 mm mannitol. The ESS signals produced by treatment with 50, 100, 800 mm mannitol, and 2 μm staurosporine are shown in (b).

is small by comparison. A larger volume loss is required to produce a comparable optical response. Furthermore, the addition of 800 mm mannitol, which has been shown to induce apoptosis in CHO cells at similar levels to 2 μm staurosporine, also produces a strong optical response. These results suggest that, while the optical effects of mannitol-induced volume decrease are similar to early effects of apoptosis induction, volume loss alone cannot explain the early optical signal produced by apoptosis inducers. It is likely that additional early ultrastructural organelle morphology changes also contribute to the early optical signal, which will be addressed in future work.

These findings are consistent with a recent study, where a weak correlation was found between changes in the ratio of wide-to-narrow angle scattering upon apoptosis induction

and cell shrinkage,[23] and alterations in mitochondria were proposed to be responsible for early scattering changes (1 h post-treatment) in cells where apoptosis was induced using staurosporine. It is possible that mitochondrial alterations during apoptosis may also contribute to the early changes in wavelength-dependent backscattering observed here, though further experiments will be necessary to determine this.

Additionally, we note that the volume measurements were made on cells that had been removed from their substrates and resuspended. Due to the normally-adherent nature of CHO cells, their morphologies are flattened [as depicted in Fig. 1(a)] during optical measurements, but are spherical once resuspended. While the flow cytometry measurements give an indication of relative volume loss, it is unclear how this volume reduction af-
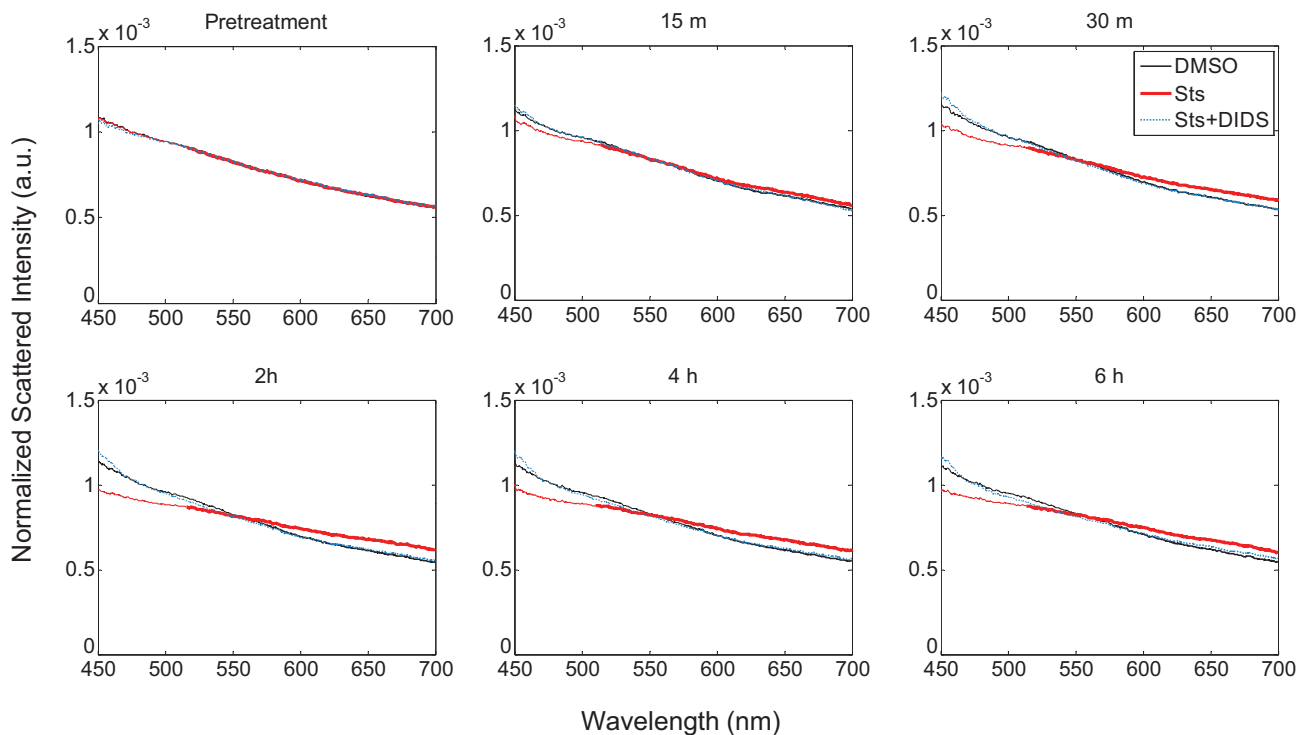
Fig. 10 Average ESS measurements of CHO cells ($n = 9$) treated with DMSO only (thin solid), staurosporine (thick solid), and staurosporine plus the chloride channel blocker DIDS (thin dotted). Control samples containing DIDS alone showed no change in scattering spectrum and are not shown.
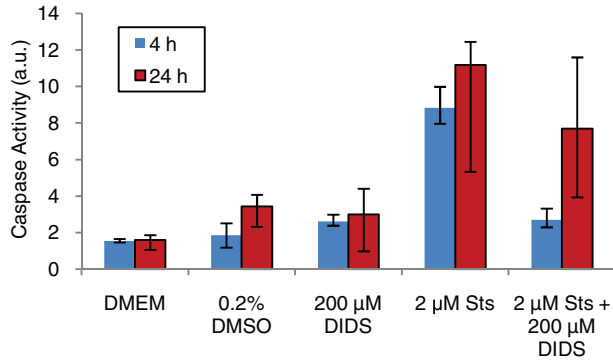
Fig. 11 Caspase-3 and caspase-7 activity ($n = 3$) as measured fluoro-metrically for an untreated culture and cells treated with DMEM only, 0.2% DMSO only, 50 μm z- 200 μm DIDS only, 2 μm staurosporine only, and 2 μm staurosporine plus 200 μm DIDS. Activity levels are shown at 4 h and 24 h.

fects the scattering properties of cells with a flattened geometry, making comparisons between absolute volume loss and absolute optical signal magnitude difficult.

Finally, during apoptosis, cells lose adherence to the substrate and rounding up of the cell is commonly observed [Fig. 1(b)]. In this case, phase contrast imaging of CHO cells treated with either 2 μm staurosporine or 400 to 800 mm mannitol show some rounding up when compared to a normally propagating culture and those treated with 50 to 200 mm mannitol (data not shown). While it is difficult to quantify the amount of rounding up that occurs in each sample, if examined qualitatively, a stronger early optical signal is observed in cultures that have rounded up. The optical properties of these rounded-up cells may differ from cells that have undergone an equivalent osmotic volume loss but retain adherence, and this may contribute to differences seen in the magnitude of the early optical signal.

3.3 Impact of Chloride Channel Inhibitor DIDS

3.3.1 ESS measurements

Figure 10 displays the average spectra of the control samples (thin solid) as well as those treated with staurosporine (thick solid) and staurosporine plus DIDS (thin dotted). Over the course of the experiment, the cells treated with staurosporine produce a scattering spectrum with all the features of a signal from an apoptotic population (see early and late scattering changes in Fig. 4). In the cells treated with staurosporine plus DIDS, however, the initial early signal is absent, resulting in a scattered spectrum indistinguishable from the culture treated with DMSO alone.

3.3.2 Caspase activity

Figure 11 shows that cells treated with staurosporine show a marked increase in caspase activity compared to the DMEM, DMSO and DIDS-only control. Staurosporine induced a clear increase in caspase activity at both 4 and 24 h, while DIDS largely blocked the increase in activity by staurosporine at 4 h and attenuated it at 24 h.
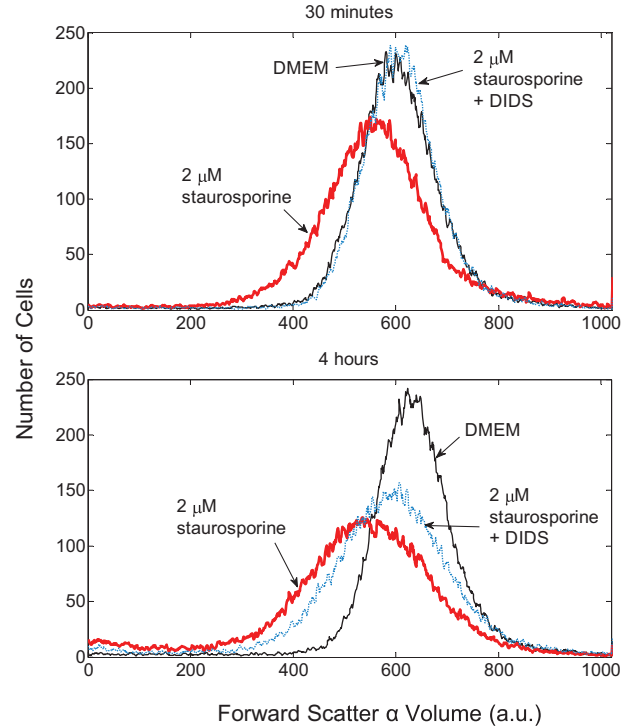
Fig. 12 Volume measurements of cell populations treated with 2μm staurosporine (thick solid), 2 μm staurosporine plus 200 μm DIDS (thin dotted), or left untreated in DMEM alone (thin solid).

3.3.3 Loss of cell volume during apoptosis

To assess the effects of staurosporine plus DIDS on cell volume, a flow cytometry analysis was performed. Volume distribution measurements from populations of 40,000 cells treated with DMEM (thin solid), 2 μm staurosporine (thick solid), or 2 μm staurosporine plus 200 μm DIDS (thin dotted) are shown in Fig. 12.

At 30 min and 4 h after staurosporine treatment, the plot of forward scattering shows the expected volume reduction and a broadening of the distribution when compared to the untreated sample. Cells treated with both staurosporine and DIDS do not show any significant loss of volume at 30 min after treatment. At 4 h, they do begin to lose some volume, though the loss is less than that of the cells treated with staurosporine alone.

3.3.4 Discussion

To ascertain the effect of the loss of cell volume on the optical signal, DIDS was used to block initial AVD in CHO cells treated with staurosporine. Volume measurements at early times confirm that the addition of DIDS maintains the initial cell volume for several hours, and then retards subsequent volume loss. Caspase assay also indicates that little caspase activity is present in the first 4 h. Taken together with the fact that volume decrease in the absence of apoptosis produces the same qualitative optical response as with apoptosis inducers, these data suggest that the early optical signal is due in part to apoptotic volume decrease.

We also note that eventual volume loss, as measured by flow cytometry, after co-treatment with DIDS occurs earlier (4 h) than changes in ESS spectra (24 h, data not shown). The reason for this discrepancy is currently unknown. As noted in Sec. 3.1.4,

the early optical effects are likely not due to AVD alone, but may include other early morphology changes that are partially masked by the AVD response. Further studies are required to identify these morphology changes, as well as how treatment with DIDS may affect the kinetics of those changes.

4 Conclusions and Future Studies

The studies presented above inform hypotheses about the biological origin of specific changes in wavelength-dependent backscattered spectra from cells undergoing apoptosis. The early ESS signal is likely due in part to water loss during AVD. Scattering changes produced by volume loss in the absence of apoptosis are qualitatively the same as the early changes in scattering upon apoptosis induction, and volume loss was confirmed by flow cytometry. Further, inhibiting volume loss with a Cl^- channel blocker eliminates the early optical signal. The magnitude of scattering changes upon apoptosis induction, however, is greater than changes caused by an equivalent osmotic volume loss. This suggests that other intracellular morphological changes also contribute to the early signal. These additional morphology changes may include alterations in mitochondrial structure or chromatin condensation below the resolution limit of optical microscopy, or the effects of cellular rounding up during apoptosis.

Early loss of cell volume is one of the most striking differences between apoptotic and necrotic cell death. Thus, cell shrinkage is a characteristic feature that allows discrimination between apoptosis and necrosis and can be considered a signature of programmed cell death.[33] Therefore, we submit that while early shrinkage is not necessarily specific to apoptosis, the associated early optical signal is also an important factor when monitoring apoptosis in cell cultures.

Additional contributions to the early scattering changes may result from other organelles. Mitochondrial changes are also implicated relatively early in the apoptotic process. Some reports indicate that mitochondria swell early in apoptosis,[15,35] while others indicate that the mitochondrial matrix condenses,[36] depending on circumstances. Some reports indicate that mitochondria fragment into multiple small units prior to, or simultaneous with, cytochrome c release and upstream of caspase activation,[37] making mitochondrial fragmentation a possible early apoptotic event. It is also possible that optical microscopy does not reveal subresolution nuclear changes in early apoptosis. In electron micrographs from the literature taken at early times (10 min) following apoptosis induction, nuclei appear as uniformly dense, chromatin-containing spheres without evidence of condensation.[38] Additionally, in our highest-resolution microscopy of stained apoptotic cells, there was no evidence of mitochondrial fragmentation at early (<6 h) time points following treatment (data not shown). Moreover, for the morphology changes of either nuclei or mitochondria, scattering theory tells us that the expected spectral change would be an increase in the slope, not a decrease.

Taken as a whole, the work presented here demonstrates that ESS can exploit morphology changes to monitor the state of apoptosis in cell cultures. It is clear, nonetheless, that further studies must be completed to develop ESS as a reliable diagnostic tool for apoptosis, particularly if it is to be used quantitatively and if it is to be translated to *in vivo* applications. Given that the early scattering changes at least partially result from cell volume decrease, the scattering model used to extract information must also be modified to account for a change in the cytoplasm's refractive index. Loss of cellular water will cause the density, and therefore, the refractive index of the cytoplasm to increase. In our current model, this corresponds to a decrease in relative refractive index of intracellular structures. At this time, it is unclear whether water loss is the only apoptotic change responsible for the early scattering changes, or if additional elements are needed. Certainly at later times, the cytoplasm remains condensed while structures condense and fragment. Further studies should be done to determine if the effect of index change is sufficient to model the early signal, and at what point the addition of changes in structure sizes is required. Additionally, the increase in index of refraction of the cytoplasm increases the relative refractive index across the cell membrane (since the index of the medium is constant). This increased index ratio, in combination with the detachment and rounding up of apoptotic cells, is consistent with an increased contribution of the whole cell to the scattered spectrum. Additional studies are required to determine the magnitude of this effect. A combination of phase-contrast imaging and finite-difference time-domain modeling may prove useful in understanding the specific effects of an increase of intracellular index on light scattering.[39–41]

Finally, it is also possible that the AVD response in CHO cells masks subtle early micromorphological changes. While AVD has been identified as a universal hallmark of apoptosis in virtually all cells,[42] if an apoptotic model can be identified that does not exhibit AVD, removal of this masking effect would allow direct assessment of those morphology changes. A possible source of these morphology changes is mitochondrial alterations during early apoptosis. Separation of mitochondrial effects from the AVD response may be achieved through simultaneous blockage of chloride channels and apoptosis induction via direct mitochondrial damage. Direct mitochondrial damage can be achieved through porphycene-induced photodamage[4] or the addition of potassium cyanide,[43] another potentially fruitful avenue for future studies.

References

1. J. F. R. Kerr, A. H. Wyllie, and A. R. Currie, "Apoptosis: a basic biological phenomenon with wide-ranging implications in tissue kinetics," *B. J. Cancer* **26**, 239–257 (1972).
2. J. M. Brown and L. D. Attardi, "The role of apoptosis in cancer development and treatment response," *N. Rev. Cancer* **5**(3), 231–237 (2005).
3. J. F. R. Kerr, C. M. Winterford, and B. V. Harmon, "Apoptosis: Its Significance in Cancer and Cancer Therapy," *Cancer* **73**(8), 2013–2026 (1994).
4. D. Kessel and Y. Luo, "Photodynamic therapy: A mitochondrial inducer of apoptosis," *Cell Death Differ.* **6**, 28–35 (1999).
5. W. Hu and J. J. Kavanagh, "Anticancer therapy targeting the apoptotic pathway," *Lancet Oncol.* **4**, 721–729 (2003).
6. S. W. Lowe and A. W. Lin, "Apoptosis in cancer," *Carcinogenesis* **21**(3), 485–495 (2000).
7. D. J. Waxman and P. S. Schwartz, "Harnessing apoptosis for improved anticancer gene therapy," *Cancer Res.* **63**, 8563–8572 (2003).

8. F. G. Blankenburg, "*In vivo* detection of apoptosis," *J. of Nuclear Med.* **49**(Supplement 2), 81S–95S (2008).

9. C. V. Remilliard and J. X.-J. Yuan, "Activation of K$^+$ channels: an essential pathway in programmed cell death," *Am. J. of Physiol. Lung Cell. Mol. Physiol.* **286**, L49–L67 (2004).

10. Y. Okada, E. Maeno, T. Shimizu, K. Dezaki, J. Wand, and S. Morishima, "Receptor-mediated control of regulatory volume decrease (RVD) and apoptotic volume decrease (AVD)," *J. Physiol.*, **532**, 3–16 (2001).

11. Y. Okada, T. Shimizu, E. Maeno, S. Tanabe, X. Wang, and N. Takahashi, "Volume-sensitive chloride channels involved in apoptotic volume decrease and cell death," *J. Membr. Biol.* **209**, 21–29 (2006).

12. E. Maeno, T. Shimizu, and Y. Okada, "Normotonic cell shrinkage induces apoptosis under extracellular low Cl- conditions in human lymphoid and epithelial cells," *Acta Physiolo.* **187**, 217–222 (2006).

13. C. D. Bortner and J. A. Cidlowski, "Apoptotic volume decrease and the incredible shrinking cell," *Cell Death Differ.* **9**, 1307–1310 (2002).

14. G. Häcker, "The morphology of apoptosis," *Cell Tissue Res.*, **301**, 5–17 (2000).

15. D. R. Green and J. C. Reed, "Mitochondria and apoptosis," *Science* **281**, 1309–1312 (1998).

16. L. Scorrano, M. Ashiya, K. Buttle, S. Weiler, S. A. Oakes, C. A. Mannella, and S. J. Korsmeyer, "A distinct pathway remodels mitochonndrial christae and mobilizes cytochrome c during apoptosis," *Dev. Cell* **2**, 55–67 (2002).

17. J. M. Adams, "Ways of dying: multiple pathways to apoptosis," *Genes Dev.* **17**, 2481–2495 (2003).

18. N. N. Boustany, S. C. Kuo, and N. V. Thakor, "Optical scatter imaging: subcellular morphometry in situ with Fourier filtering," *Opt. Lett.* **26**(14), 1063–1065 (2001).

19. N. N. Boustany, Y. C. Tsai, B. Pfister, W. M. Joiner, G. A. Oyler, and N. V. Thakor, "BCL-x(L)-dependent light scattering by apoptotic cells," *Biophys. J.* **87**(6), 4163–4171 (2004).

20. J. D. Wilson, B. R. Giesselman, S. Mitra, and T. H. Foster, "Lysosome-damage-induced scattering changes coincide with release of cytochrome c," *Opt. Lett.* **32**(17), 2517–2519 (2007).

21. C. S. Mulvey, A. L. Curtis, S. K. Singh, and I. J. Bigio, "Elastic scattering spectroscopy as a diagnostic tool for apoptosis in cell cultures," *IEEE J. Sel. Top. Quantum Electron.* **13**(6), 1663–1670 (2007).

22. C. S. Mulvey, C. A. Sherwood, and I. J. Bigio, "Wavelength-dependent backscattering measurements for quantitiative real-time monitoring of apoptosis in living cells," *J. Biomed. Opt.* **14**(6), 064013 (2009).

23. J.-Y. Zheng and N. N. Boustany, "Alterations in the characteristic size distributions of subcellular scatterers at the onset of apoptosis: effect of Bcl-xL and Bax/Bak," *J. Biomed. Opt.* **15**(4), 045002 (2010).

24. H. Fang, M. Ollero, E. Vitkin, L. M. Kimerer, P. B. Cipolloni, M. M. Zaman, S. D. Freedman, I. J. Bigio, I. Tizkan, E. B. Hanlon, and L. T. Perelman, "Noninvasive Sizing of Subcellular Organelles with Light Scattering Spectroscopy," *IEEE J. Sel. Top. Quantum Electron.* **9**, 267–276 (2003).

25. H. Fang, L. Qiu, M. M. Zaman, E. Vitkin, S Salahuddin, C. Andersson, L. M. Kimerer, P. B. Cipolloni, M. D. Modell, B. S. Turner, S. E. Keates, I. J. Bigio, I. Itzkan, S. D. Freedman, R. Bansil, E. B. Hanlon, and L. T. Perelman, "Confocal light absorption and scattering spectroscopic (CLASS) microscopy," *Appl. Opt.* **46**, 1760–1769 (2007).

26. I. Itzkan, L. Qui, H. Fang, M. M. Zaman, E. Vitkin, I. C. Ghiran, S. Salahuddin, M. D. Modell, C. Andersson, L. M. Kimerer, P. B. Cipolloni, K.-H. Lim, S. D. Freedman, I. J. Bigio, B. P. Sachs, E. B. Hanlon, and L. T. Perelman, "Confocal light absorption and scattering spectroscopic (CLASS) microscopy monitors organelles in live cells with no exogenous labels," *Proc. Natl. Acad. Sci. U.S.A* **104**, 17255–17260 (2007).

27. J.-L. Castagner and I. J. Bigio, "Polar nephelometer based on a rotational confocal imaging setup," *Appl. Opt.* **45**, 2232–2239 (2006).

28. J.-L. Castagner and I. J. Bigio, "Particle sizing with a fast polar nephelometer," *Appl. Opt.* **46**, 527–532 (2007).

29. J. R. Mourant, J. P. Freyer, A. H. Hielscher, A. A. Eick, D. Shen, and T. M. Johnson, "Mechanisms of light scattering from biological cells relevant to noninvasive optical-tissue diagnostics," *Appl. Opt.* **37**, 3586–3593 (1998).

30. J. R. Mourant, M. Canpolat, C. Brocker, O. Esponda-Ramos, T. M. Johnson, A. Matanock, K. Stetter, and J. P. Freyer, "Light scattering from cells: The contribution of the nucleus and the effects of proliferative status," *J. Biomed. Opt.* **5**(2), 131–137 (2000).

31. A. M. Porcelli, A. Ghelli, C. Zanna, P. Valente, S. Ferroni, and M. Rugulo, "Apoptosis induced by staurosporine in ECV304 cells requires cell shrinkage and upregulation of Cl$^-$ conductance," *Cell Death Differ.* **11**, 655–662 (2004).

32. S. Rello, J. C. Stockert, V. Moreno, A. Gámez, M. Pacheco, A. Juarranz, M. Cañete, and A. Villanueva, "Morphological criteria to distinguish cell death induced by apoptotic and necrotic treatments," *Apoptosis* **10**, 201–208 (2005).

33. M. Gomez-Angelats and J. A. Cidlowski, "Cell volume control and signal transduction in apoptosis," *Toxicol. Pathol.* **30**(5), 541–551 (2002).

34. N. J. Ernest, C. W. Habela, and H. Sontheimer, "Cytoplasmic condensation is both necessary and sufficient to induce apoptotic cell death," *J. Cell Sci.* **121**, 290–297 (2007).

35. M. G. Vander Heiden, N. S. Chandel, E. K. Williamson, P. T. Schumacker, and C. B. Thompson, "Bcl-xL regulates the membrane potential and volume homeostasis of mitochondria," *Cell* **91**, 627–637 (1997).

36. S. Desagher and J.-C. Martinou, "Mitochondria as the central control point of apoptosis," *Trends Cell Biol.* **10**, 369–377 (2000).

37. D. Suen, K. L. Norris, and R. J. Youle, "Mitochondrial dynamics and apoptosis," *Genes Dev.* **22**, 1577–1590 (2008).

38. M. J. Arrends, R. G. Morris, and A. H. Wyllie, "Apoptosis: The role of the endonuclease," *Am. J. Pathol.* **136**(3), 593–608 (1990).

39. C. E. Rommel, C. Dierker, L. Schmidt, S. Przibilla, G. von Bally, B. Kemper, and J. Schnekenburger, "Contrast-enhanced digital holographic imaging of cellular structures by manipulating the intracellular refractive index," *J. Biomed. Opt.* **15**(4), 041509 (2010).

40. S. Tanev, V. V. Tuchin, and P. Paddon, "Cell membrane and gold nanoparticles effects on optical immersion experiments with normal and cancerous cells: finite-difference time-domain modeling," *J. Biomed. Opt.* **11**(6), 064037 (2006).

41. S. Tanev, W. Sun, J. Pond, V. V. Tuchin, and V. P. Zharov, "Flow cytometry with gold nanoparticles and their clusters as scattering contrast agents: FDTD simulation of light-cell interaction," *J. Biophotonics* **2**(8–9), 505–520 (2009).

42. L. Wei, A. Y. Xiao, C. Jin, A. Yang, Z. Y. Lu, and S. P. Yu, "Effects of chloride and potassium channel blockers on apoptotic cell shrinkage and apoptosis in cortical neurons," *Eur. J. Physiol.*, **448**, 325–334 (2004).

43. Y. Shou, L. Li, K. Prabhakaran, J. L. Borowitz, and G. E. Isom, "p38 mitogen-activated protein kinase regulates bax translocation in cyanide-induced apoptosis," *Toxicol. Sci.* **75**, 99–107 (2003).